

because of known fabrication issues which will be solved in a second fabrication run later this year.

This work was supported by ERC project NOLIMITS and the Marie Curie Actions in the Career Integration Grant.

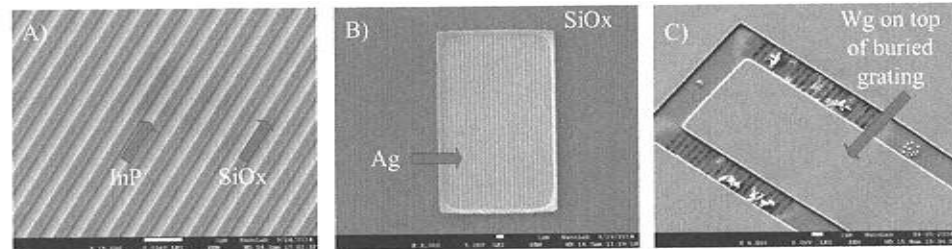


Figure 2. SEM pictures of the gratings fabrication process. Top left shows patterned SiO₂ gratings (2nd EBL), top right shows gratings covered with Ge and Ag (3rd EBL). Bottom center shows the tapered waveguide patterned on the InP membrane over the buried metal gratings (4th EBL).

References

- [1] J. van der Tol, R. Zhang, J. Pello, F. Bordas, G. Roelkens, H. Ambrosius, P. Thijs, F. Karouta, and M. Smit, *IET Optoelectron.* 5, 218 (2011).
- [2] J. Yao, X. Zheng, G. Li, I. Shubin, H. Thacker, Y. Luo, K. Raj, J. E. Cunningham, and A. V. Krishnamoorthy, "Grating-coupler based low loss optical interlayer coupling", *Proceedings of IEEE International Conference on Group IV Photonics*, pp. 383-385 (2011).
- [3] V. Dolores-Calzadilla, A. Higuera-Rodriguez, D. Heiss, and Meint Smit, "Efficient metal grating coupler for membrane-based integrated photonics", *IPR conference from OSA 2014, San Diego C.A.* (July-2014).
- [4] F. Van Laere, G. Roelkens, M. Ayre, J. Schrauwen, D. Taillaert, D. Van Thourhout, T. F. Kraus, and R. Baets, "Compact and highly efficient grating coupler between optical fiber and nanophotonic waveguides", *J. Light. Technol.* 25, 151-156 (2007).
- [5] S. Scheerlinck, J. Schrauwen, F. V. Laere, D. Taillaert, D. Van Thourhout, and R. Baets, "Efficient, broadband and compact metal gratings couplers for silicon-on-insulator waveguides", *Opt. Exp.* 15, 9625-9630 (2007).
- [6] P. Lin, C.-Y. Wu, and P.-T. Lee, "Buried metal grating for vertical fiber-waveguide coupling with high directionality", in *Advanced Photonics Congress, OSA Technical Digest (Optical Society of America, 2012)*, paper IM4B.6.
- [7] S. Keyvaninia, S. Verstuyft, F. Lelarge, G.-H. Duan, S. Messaoudene, J. M. Fedeli, T. De Vries, B. Smalbrugge, J. Bolk, M. Smit, D. Van Thourhout, and G. Roelkens, "Heterogeneously integrated III-V/Si multi-wavelength laser based on a ring resonator array multiplexer", in *Asia Communications and Photonics Conference, OSA Technical Digest (Optical Society of America, 2012)*, paper PAF4A.3.

Fabrication and Thermal Tolerant all-Silicon Wavelength Filtering Devices

Sarvagya Dwivedi¹, Herbert D'heer¹ and Wim Bogaerts^{1,2}

¹Photonics Research Group, Department of Information Technology Ghent University - imec, Center for Nano- and Biophotonics, Sint-Pietersnieuwstraat 41, B-9000 Ghent, Belgium

²now also with: Lucedra Photonics, Dendermonde, Belgium

Silicon on Insulator (SOI) is getting a mature platform for dense integration of wavelength filtering devices due to the high index contrast of silicon. This brings a weakness to this platform, i.e. extremely precise fabrication is required, especially for these devices. High thermo-optic coefficient of silicon ($1.86 \times 10^{-4} K^{-1}$) is another issue to this platform since it affects device performance because of ambient thermal fluctuations (shift in resonance by 80 – 100 pm/K). In this work we propose a method and tested it on a Mach-Zehnder interferometer (MZI) filter and showed indeed it is possible to improve the tolerances to fabrication (waveguide geometry) and ambient thermal variations. The method is based on different mode confinement in either arm of the devices and it can be achieved by different waveguide widths or polarizations or both at the same time. The fabricated device shows a shift of less than ± 65 pm/nm in line-width variations and a smaller than ± 15 pm/K in thermal variations over a wavelength range of 40 nm which is more than a 10 times improvement with respect to conventional devices.

Introduction

Silicon on Insulator (SOI) is a promising platform because of its high refractive index contrast that enables dense integration of micron – sized photonic integrated circuits. The high index contrast and submicron waveguide dimensions can translate a small change in the waveguide width (shift in resonance by 1 nm/nm) and height (shift in resonance by 1.5 nm/nm) into a strong change in the effective refractive index [1], as shown in Fig. 1. This brings a weakness to this platform, i.e. extremely precise fabrication is required, especially for the wavelength filtering devices. While fabrication technology improves systematically, the required fabrication control will ultimately dictate the yield of larger circuits. Another important issue is the high thermo-optic coefficient of silicon ($1.86 \times 10^{-4} K^{-1}$) which affects device performance because of ambient temperature variations (shift in resonance by 80 – 100 pm/K). Fabrication and thermal variations can be actively compensated (e.g. with thermal tuning), but this will drive up power consumption and complicate the device with active control circuitry. While fabrication technology is systematically improving, the required fabrication control will ultimately dictate the yield of larger circuits. Pre-fabrication or post-fabrication trimming [2] of the components can be used to correct the effects of the "last nanometer" fabrication offsets. However it comes with a significantly increased cost of the whole fabrication process. Other techniques involve the introduction of compensating materials such as polymers or TiO₂ [3, 4], but this again complicates fabrication and also faces CMOS compatibility and reliability issues. In this paper, we present a technique to make a wavelength filter tolerant to line-width variations by design, without changing the fabrication process itself. We demonstrate a fabrication

tolerant MZI filter by using a different mode confinement in the two arms of the filter. This can be accomplished by using waveguides of different widths, or using different polarizations in the waveguides. This technique has already been used to make filters tolerant to thermal variations [3], but here we extend it to tolerance to fabrication variations and even to multiple effects (waveguide width and thermal variations) at the same time.

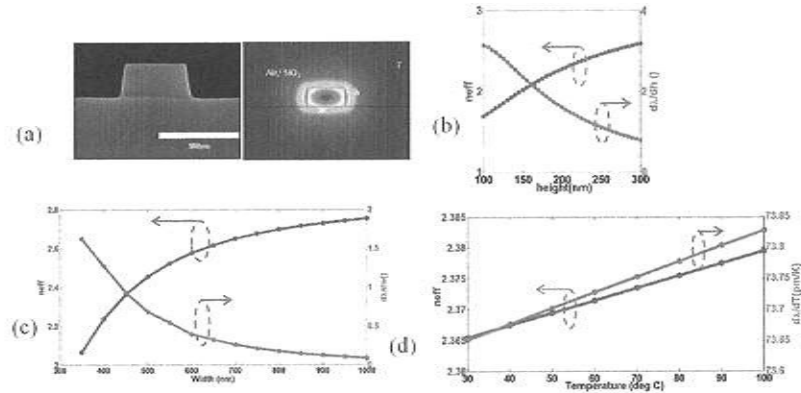


Fig. 1. (a) SEM image and mode profile of waveguide, (b) Sensitivity of spectrum position to height, (c) width and, (d) temperature variation for a conventional FIR filter with waveguide width 450 nm and thickness 220 nm at a wavelength of 1550 nm

Proposed Solution

The wavelength sensitivity of an FIR filtering device to parameter X can be expressed as

$$\frac{d\lambda}{dX} = \frac{\lambda_m}{n_g} \frac{dn_{eff}}{dX} \quad (1)$$

where X can be replaced by the waveguide width (w), height (h), temperature (T) or any other influence. We assume here that the influence affects the entire device uniformly. λ_m is the wavelength of operation, and n_g is the group index. To compensate the wavelength sensitivity due to the fabrication variations, we introduce design variations such as different waveguide width in each arm. The modified expression for the sensitivity then becomes

$$\frac{d\lambda}{dX} = \frac{\lambda_m}{n_{g1}L_1 - n_{g2}L_2} \left(L_1 \frac{dn_{eff1}}{dX} - L_2 \frac{dn_{eff2}}{dX} \right) \rightarrow 0 \quad (2)$$

which we try to minimize. For a device tolerant to width variations the condition for zero sensitivity at wavelength λ_0 and for a given free spectral range (FSR) becomes

$$\frac{L_1}{L_2} = \frac{dn_{eff2}/dw}{dn_{eff1}/dw} \quad (3)$$

For the filter to be width tolerant the length ratio of the arms should be inversely proportional to the sensitivity of the effective index of the waveguides in both arms. The assumption we make here is that the linewidth change induced by the fabrication process is similar for the waveguides in the two arms. This is generally true if the linewidth change is caused by global or long-range effects, such as lithographic dose variation or a change in etch rate, and the device is sufficiently compact.

To make the devices fabrication as well as thermally tolerant we introduce orthogonal

polarizations (TE and TM) in the two arms of the filter. For width along with thermal tolerant, the wavelength sensitivity with respect to temperature ($\frac{d\lambda}{dT}$) becomes zero and (2) should satisfy

$$L_{TM} \frac{dn_{eff,TM}}{dT} = L_{TE} \frac{dn_{eff,TE}}{dT} \quad (4)$$

where L_{TM} , L_{TE} and $\frac{dn_{eff,TM}}{dT}$, $\frac{dn_{eff,TE}}{dT}$ are the length of TM, TE arm and their corresponding waveguide thermo-optic coefficients (TO). The combined condition of being tolerant to width and temperature at wavelength λ_0 and at temperature T_0 for a given FSR becomes

$$\frac{L_{TE}}{L_{TM}} = \frac{TO_{TM}}{TO_{TE}} = \frac{dn_{eff,TM}/dw}{dn_{eff,TE}/dw} \quad (5)$$

Physically it means that a variation in width or temperature gives an identical change in phase in each arm.

Design and Fabrication

We have designed the devices using the IPKISS parametric design framework [4]. To demonstrate the width and thermal tolerant behavior as given in equation (5), the designed TM and TE nominal width are 490 nm, and 522 nm and their corresponding lengths are 180 μm and 87 μm , respectively for an FSR of around 10 nm. The SEM picture of the fabricated device is shown in Fig. 5. The device uses a splitter polarization rotator (SPR) which splits the light into two equal parts and at the same time rotates the polarization in one arm. This directional coupler device is based on the phase matching condition of thinner TE waveguide and thicker TM waveguide ($n_{effTE} = n_{effTM}$). The same is used at the output to combine the two modes. The fabricated devices are shown in Fig. 2.

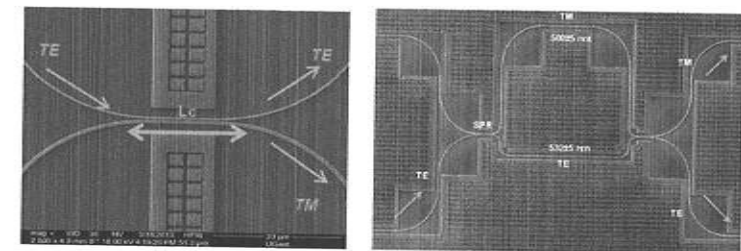


Fig. 2 (a) SEM image fabricated SPR and (b) fabricated MZI with SPR

Measurements

We characterized first the SPR separately. The transmission spectrum of the SPR for cross coupling is shown in figure 3 for different coupling lengths. It shows that the coupling length of 10 μm is closest to the desired 3 dB of power transfer from the input to the TM mode in the other arm. A variation of 1 μm from this length shows a 0.5 dB variation in transmission in the lower wavelength side of the spectrum. The coupler design is sufficiently tolerant such that a width variation of couple of nanometers in fabrication will not have a detrimental impact. The measured SEM width of the fabricated device is 502 \pm 5 nm in TM arm and 534 \pm 5 nm in TE arm. The simulated

transmission using the device parameters from SEM are shown in figure 4(a). Measurements are performed on nominal width device at three different temperatures, and 50°C on a nominal width device and on varying width devices of ±10 nm. The six measured transmission spectra are shown in figure 4(b). The thermal insensitive point is situated around 1525 nm.

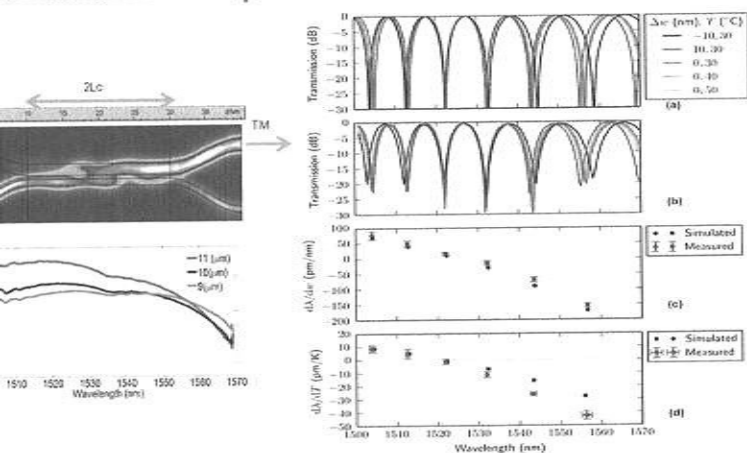


Figure 4: (a) Simulated intensity profile for the calculated cross coupling length from the input TE mode to the output TM mode and transmission of the SPR test structure for different coupling lengths. Fig4 (a) Simulated spectra of optimized design with 0 nm width offset and at 30, 40 and 50 °C, (b) Measured transmission, (c) width sensitivity variation ($d\lambda/dw$) and (d) thermal sensitivity ($d\lambda/dT$) simulated and measured

The device shows a width sensitivity of less than ±65 pm/nm with a standard deviation of about 15 pm/nm measured over four devices with width offsets of ±10 nm and thermal sensitivity of less than ±15 pm/K with a standard deviation of about 5 pm/K over the wavelength range of 40 nm. The simulated and measured results as thermal sensitivity is shown in Figs. 4(c) and (d). The width sensitivity goes from positive to negative on the different sides of the insensitive point i.e. a positive width offset will result in either a blue-shift or a red-shift. A similar behavior can be observed when varying the temperature of the device.

Conclusion

We have proposed and demonstrated width and thermal tolerant compact device with width sensitivity smaller than ±65 pm/nm and thermal sensitivity smaller than ±15 pm/K over 40 nm wavelength range. These devices can be used for higher order WDM filters like in integrated photonic devices (IPDs).

References

1. S. J. Lee, et al., "Sub-nanometer linewidth uniformity in silicon nano-photonics waveguide devices using CMOS technology," *IEEE J. Sel. Top. Quantum Electron.*, vol. 16, pp.316 – 324, Jan. 2010.
2. J. M. M. van den Brink, et al., "Trimming of silicon ring resonator by electron beam induced compaction and strain," *Opt. Exp.*, vol. 16, pp. 4743, Mar. 2008
3. J. M. M. van den Brink, et al., "A compact all-silicon temperature insensitive filter for WDM and bio-sensing applications," *IEEE Tech. Lett.*, vol. 25, pp.2167 – 2170, Nov. 2013
4. J. M. M. van den Brink, et al., "Integrated design for integrated photonics: From the physical to the circuit level and back," *Proc. SPIE*,

Gain characterization of a lattice-engineered potassium double tungstate thin film with 57.5 at.% ytterbium concentration

Y.S. Yong^{1,2}, S. Aravazhi¹, S.A. Vázquez-Córdova^{1,2}, S.M. García-Blanco^{1,2}, and M. Pollnau^{1,3}

¹ Integrated Optical MicroSystems Group, MESA+ Institute for Nanotechnology, University of Twente, P.O. Box 217, 7500 AE Enschede, The Netherlands

² Optical Sciences Group, MESA+ Institute for Nanotechnology, University of Twente, P.O. Box 217, 7500 AE Enschede, The Netherlands

³ Department of Materials and Nano Physics, School of Information and Communication Technology, KTH–Royal Institute of Technology, Electrum 229, Isafjordsgatan 22–24, 16440 Kista, Sweden

We report the measurement results on an ytterbium-activated potassium gadolinium double tungstate (KGW) thin film grown onto a potassium yttrium double tungstate (KYW) substrate. The 57.5 at.% Yb-doped active layer, in which the material composition reaches the upper limit of Yb concentration lattice matched to the KYW substrate, was grown by liquid phase epitaxy and polished to ~32 μm thickness. The measured lifetime indicates that lifetime quenching is rather insignificant. Besides, a high gain per unit length of about 1050 dB/cm was obtained. The results show that this material is favorable for the fabrication of waveguide amplifiers for short optical interconnects requiring compact device footprint.

Introduction

Rare-earth-doped amplifiers are well known for their capability of supporting high-gain, high-bit rate, and broadband amplification. However, it remains a great challenge to reduce the length of these devices to realize on-chip waveguide amplifiers for emerging footprint-limited applications, such as photonic integrated circuits, optical sensing devices, and optical backplane systems, to name just a few. Typical rare-earth-doped waveguide amplifiers possess a material gain of only a few dB/cm, mainly due to the small emission cross-sections resulting from the combination of a long emission lifetime and a fast atomic dephasing time [1], and the limited dopant concentration of rare-earth ions in the host materials. Therefore, device lengths of tens of centimeters are usually needed for practical amplification.

In order to achieve high gain per unit length, the amplifier material must exhibit both high transition cross-sections and high doping concentration [2]. Therefore, in this work, a lattice-engineered approach [3,4] is employed to maximize the concentration of ytterbium (Yb) ions in a potassium double tungstate [5] crystalline film grown onto a substrate of potassium yttrium double tungstate, KY(WO₄)₂ (denoted as KYW hereafter). The method was applied successfully to fabricate a 47.5 at.% Yb-doped potassium double tungstate waveguide amplifier with ~1000 dB/cm gain at 981 nm [2]. Here we report the successful growth of 57.5 at.% Yb-doped layers of potassium gadolinium double tungstate, KGd(WO₄)₂ (denoted as KGW hereafter) onto KYW. Characterization results show that the thin-film gain material does not exhibit significant lifetime quenching. Apart from that, a gain per unit length of more than 1000 dB/cm is obtained from pump-probe gain measurements.